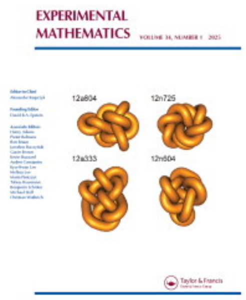

Taylor & Francis
Taylor & Francis Group

Experimental Mathematics

ISSN: (Print) (Online) Journal homepage: www.tandfonline.com/journals/uexm20

Data-Scientific Study of Kronecker Coefficients

Kyu-Hwan Lee

To cite this article: Kyu-Hwan Lee (01 May 2025): Data-Scientific Study of Kronecker Coefficients, Experimental Mathematics, DOI: 10.1080/10586458.2025.2490576

To link to this article: https://doi.org/10.1080/10586458.2025.2490576

EXPERIMENTAL MATHEMATICS
2025, VOL. 00, NO. 0, 1–14
https://doi.org/10.1080/10586458.2025.2490576

Data-Scientific Study of Kronecker Coefficients

Kyu-Hwan Lee[a,b]

[a]Department of Mathematics, University of Connecticut, Storrs, CT, USA; [b]Korea Institute for Advanced Study, Seoul, Republic of Korea

ABSTRACT
We take a data-scientific approach to study whether Kronecker coefficients are zero or not. Motivated by principal component analysis and kernel methods, we define *loadings* of partitions and use them to describe a sufficient condition for Kronecker coefficients to be nonzero. The results provide new methods and perspectives for the study of these coefficients.

KEYWORDS
Kronecker coefficients; principal component analysis; kernel methods

1. Introduction

In recent years, there has been much discussion about the potential for AI and machine learning to change mathematics research (e.g., [5, 7, 27]). Numerous examples demonstrate machine learning's ability to discern patterns in mathematical datasets (e.g., [1, 6, 8, 12–15, 19]). The recent discovery [16] of a new phenomenon, called *murmuration*, illustrates the significant potential of considering mathematical objects within the framework of data science. All these developments remind us of how fruitful it has been to study datasets in modern mathematics—even long before the advent of machine learning. For instance, the prime number theorem, conjectured at the end of the 18th century, and the Birch–Swinnerton-Dyer conjecture, formulated in the mid-20th century, are all results of investigating certain datasets.

The goal of this paper is to apply this paradigm of mathematics research to representation theory. One of the primary objectives in representation theory is to decompose a representation into its irreducible components, with algebraic combinatorics providing a vital and practical method for describing this decomposition. A prototypical example is the decomposition of the tensor product of two irreducible representations of the general linear group $\mathrm{GL}_N(\mathbb{C})$, where the Littlewood–Richardson rule completely describes the decomposition using skew semi-standard tableaux.

Surprisingly enough, there has been no similar success with the symmetric group until now. Let $\mathfrak{S}_n$ be the symmetric group of degree n. The irreducible representations S_λ of $\mathfrak{S}_n$ over $\mathbb{C}$ are parameterized by partitions λ of n, written as $\lambda \vdash n$. The tensor product of two irreducible representations S_λ and S_μ ($\lambda, \mu \vdash n$) is decomposed into a sum of irreducible representations:

$$S_\lambda \otimes S_\mu = \bigoplus_{\nu \vdash n} g^{\nu}_{\lambda,\mu} S_\nu \quad (g^{\nu}_{\lambda,\mu} \in \mathbb{Z}_{\geq 0}). \tag{1.1}$$

The decomposition multiplicities $g^{\nu}_{\lambda,\mu}$ are called the *Kronecker coefficients*.

In stark contrast to the Littlewood–Richardson coefficients for $\mathrm{GL}_N(\mathbb{C})$, no combinatorial description has been known for $g^{\nu}_{\lambda,\mu}$ since Murnaghan [21] initially posed the question in 1938, and it is still considered as one of the main problems in the combinatorial representation theory. Only partial results are available due to Remmel [24], Ballantine–Orellana [2], Remmel–Whitehead [25], Blasiak–Mulmuley–Sohoni [3], and Blasiak [4]. Recently, the coefficients $g^{\nu}_{\lambda,\mu}$ have also been studied from the perspective of computational complexity. Notably, Ikenmeyer, Mulmuley and Walter [17] demonstrated that determining whether a given Kronecker coefficient is nonzero is NP-hard. Additionally, Pak and Panova [22, 23] have made other significant contributions to this topic.

In the previous article [20], we applied standard machine learning tools to datasets of the Kronecker coefficients, and observed that the trained classifiers attained high accuracies ($> 98\%$) in determining whether Kronecker coefficients are zero or not. The outcomes clearly suggest that further data-scientific analysis may reveal new structures in the datasets of the Kronecker coefficients. In this paper, we indeed find new structures; more precisely, we adopt ideas from principal component analysis (PCA) and kernel methods to define the *similitude* matrix and the *difference* matrix for the set $\mathcal{P}(n)$ of partitions of n. Then we introduce *loadings* of the partitions in terms of eigenvectors associated to the largest eigenvalues of these matrices, and use the loadings to describe a sufficient condition for the Kronecker coefficients to be nonzero. This condition can be used very effectively. See equation (4.1) and Example 4.1 below it.

The observations made in this paper are purely data-scientific and experimental, and no attempts are undertaken to prove them using representation theory. Also, it should be noted that our sufficient condition does not cover the *middle part* where loadings for zero and nonzero Kronecker coefficients overlap. Since our method is a variation of PCA, it is essentially linear. In order to cover the

CONTACT Kyu-Hwan Lee khlee@math.uconn.edu Department of Mathematics, University of Connecticut, Storrs, CT 06269, USA.

middle part, it is likely that one needs to take a nonlinear approach. The aforementioned high accuracies reported in [20] indicate that efficient strategies may be developed to go much deeper into the middle part.

After this introduction, in Section 2, we define the similitude and difference matrices and the loadings of partitions. In Section 3, we investigate the probabilistic distributions of loadings. In the final section, we consider the minimum values of the loadings to determine whether the Kronecker coefficients are zero or nonzero. In Appendix, we tabulate the loadings of partitions in $\mathcal{P}(n)$ for $6 \le n \le 12$.

2. Similitude and difference matrices

Recall the definition of the Kronecker coefficient from (1.1). The coefficients satisfy natural symmetries, as described in the following lemma.

Lemma 2.1. [9, p.61] Let $\lambda, \mu, \nu \vdash n$. Then the Kronecker coefficients $g^{\nu}_{\lambda,\mu}$ are invariant under the permutations of λ, μ, ν. That is, we have

$$g^{\nu}_{\lambda,\mu} = g^{\nu}_{\mu,\lambda} = g^{\mu}_{\lambda,\nu} = g^{\mu}_{\nu,\lambda} = g^{\lambda}_{\mu,\nu} = g^{\lambda}_{\nu,\mu}.$$

For a partition $\lambda = (\lambda_1 \ge \lambda_2 \ge \cdots)$ of n, define $d_\lambda := n - \lambda_1$, called the *depth* of λ. The following theorem provides a necessary condition for the Kronecker coefficient $g^{\nu}_{\lambda,\mu}$ to be nonzero. Other necessary conditions for $g^{\nu}_{\lambda,\mu} \neq 0$, which generalize Horn inequalities, can be found in [26]. We will describe a sufficient condition for for $g^{\nu}_{\lambda,\mu} \neq 0$ in this paper.

Theorem 2.2. [18, Theorem 2.9.22] If $g^{\nu}_{\lambda,\mu} \neq 0$ then

$$|d_\lambda - d_\mu| \le d_\nu \le d_\lambda + d_\mu. \tag{2.1}$$

Now, for $n \in \mathbb{Z}_{>0}$, let $\mathcal{P}(n)$ be the set of partitions of n as before. We identify each element λ of $\mathcal{P}(n)$ with a sequence of length n by appending as many 0-entries as needed. We also consider $\mathcal{P}(n)$ as an ordered set by the lexicographic order.

Example 2.3. When $n = 6$, we have

$$\begin{aligned}\mathcal{P}(6) = \{&(6,0,0,0,0,0), (5,1,0,0,0,0), (4,2,0,0,0,0), (4,1,1,0,0,0),\\ &(3,3,0,0,0,0), (3,2,1,0,0,0), (3,1,1,1,0,0), (2,2,2,0,0,0),\\ &(2,2,1,1,0,0), (2,1,1,1,1,0), (1,1,1,1,1,1)\}.\end{aligned}$$

For notational simplicity, when the same part is repeated more than three times, we may abbreviate it into an exponent. For example, $(2,1,1,1,1,1)$ may be written as $(2,1^5)$. The size of the set $\mathcal{P}(n)$ will be denoted by $p(n)$, and the set of triples $\mathbf{t} = (\lambda, \mu, \nu)$ of partitions of n will be denoted by $\mathcal{P}(n)^3 := \mathcal{P}(n) \times \mathcal{P}(n) \times \mathcal{P}(n)$. A partition is depicted by a collection of left-justified rows of boxes. For example, partition $(5,4,1)$ is depicted by 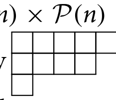. The *conjugate* or *transpose* of a partition is defined to be the flip of the original diagram along the main diagonal. Hence the conjugate of $(5,4,1)$ is $(3,2,2,2,1)$ as you can see below:

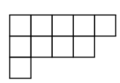 $\longleftrightarrow$ 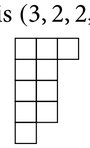

Let P_n be the $p(n) \times n$ matrix having elements of $\mathcal{P}(n)$ as rows, and define the $p(n) \times p(n)$ symmetric matrix

$$\mathsf{Y}_n := \mathsf{P}_n \mathsf{P}_n^{\top}.$$

The matrix Y_n will be called the *similitude* matrix of $\mathcal{P}(n)$.

Example 2.4. When $n = 6$, we obtain

$$\mathsf{P}_6 = \begin{bmatrix} 6&0&0&0&0&0\\ 5&1&0&0&0&0\\ 4&2&0&0&0&0\\ 4&1&1&0&0&0\\ 3&3&0&0&0&0\\ 3&2&1&0&0&0\\ 3&1&1&1&0&0\\ 2&2&2&0&0&0\\ 2&2&1&1&0&0\\ 2&1&1&1&1&0\\ 1&1&1&1&1&1 \end{bmatrix} \quad \text{and} \quad \mathsf{Y}_6 = \begin{bmatrix} 36&30&24&24&18&18&18&12&12&12&6\\ 30&26&22&21&18&17&16&12&12&11&6\\ 24&22&20&18&18&16&14&12&12&10&6\\ 24&21&18&18&15&15&14&12&11&10&6\\ 18&18&18&15&18&15&12&12&12&9&6\\ 18&17&16&15&15&14&12&12&11&9&6\\ 18&16&14&14&12&12&12&10&10&9&6\\ 12&12&12&12&12&12&10&12&10&8&6\\ 12&12&12&11&12&11&10&10&10&8&6\\ 12&11&10&10&9&9&9&8&8&8&6\\ 6&6&6&6&6&6&6&6&6&6&6 \end{bmatrix}.$$

Note that an entry $y_{\lambda,\mu}$ of $\mathsf{Y}_n = [y_{\lambda,\mu}]$ is indexed by $\lambda, \mu \in \mathcal{P}(n)$.

Since the matrix Y_n is symmetric, all its eigenvalues are real. Moreover, the Perron–Frobenius theorem [10, Section III.2] tells us that Y_n has a unique eigenvalue of largest magnitude and that the corresponding eigenvector can be chosen to have strictly positive components.

Definition 2.5. Let $\mathbf{v} = (v_\lambda)_{\lambda\in\mathcal{P}(n)}$ be an eigenvector of the largest eigenvalue of Y_n such that $v_\lambda > 0$ for all $\lambda \in \mathcal{P}(n)$. Denote by $v_{\max}$ (resp. $v_{\min}$) a maximum (resp. minimum) of $\{v_\lambda\}_{\lambda\in\mathcal{P}(n)}$. Define

$$a_\lambda \coloneqq 100 \times \frac{v_\lambda - v_{\min}}{v_{\max} - v_{\min}} \quad \text{for } \lambda \in \mathcal{P}(n).$$

The value a_λ is called the *a-loading* of partition $\lambda \in \mathcal{P}(n)$.

The above definition presents a novel concept in the exploration of Kronecker coefficients. However, when n is large, one might wonder how to compute an eigenvector of the largest eigenvalue of Y_n. The direct computation of eigenvalues can be computationally intensive. For an $N \times N$ matrix, it is known that direct computations of eigenvalues have a time complexity of $O(N^3)$.

An efficient algorithm to calculate an eigenvector $\mathbf{v}$ in Definition 2.5 is the *power iteration*: Let $\mathbf{v}_0 = (1, 0, \ldots, 0)^\top$ be the first standard column vector. Inductively, for $k = 0, 1, 2, \ldots$, define

$$\mathbf{v}_{k+1} = \frac{\mathsf{Y}_n\mathbf{v}_k}{\|\mathsf{Y}_n\mathbf{v}_k\|_2},$$

where $\|(x_1, x_2, \ldots, x_n)^\top\|_2 = (\sum_{i=1}^n x_i^2)^{1/2}$. Then the limit

$$\mathbf{v} = \lim_{k\to\infty} \mathbf{v}_k$$

is an eigenvector of the largest eigenvalue of Y_n.

Example 2.6. When $n = 6$, we have

$$\begin{aligned}
\mathbf{v}_1 &\approx (0.5203, 0.4336, 0.3468, 0.3468, 0.2601, 0.2601, 0.2601, 0.1734, 0.1734, 0.1734, 0.0867)^\top,\\
\mathbf{v}_2 &\approx (0.4514, 0.4022, 0.3530, 0.3377, 0.3038, 0.2885, 0.2670, 0.2240, 0.2178, 0.1934, 0.1188)^\top,\\
\mathbf{v}_3 &\approx (0.4441, 0.3985, 0.3530, 0.3366, 0.3074, 0.2910, 0.2678, 0.2291, 0.2222, 0.1957, 0.1225)^\top,\\
\mathbf{v}_4 &\approx (0.4434, 0.3982, 0.3529, 0.3365, 0.3077, 0.2913, 0.2678, 0.2296, 0.2226, 0.1960, 0.1229)^\top,\\
\mathbf{v}_5 &\approx (0.4433, 0.3981, 0.3529, 0.3365, 0.3077, 0.2913, 0.2678, 0.2297, 0.2226, 0.1960, 0.1229)^\top,\\
\mathbf{v}_6 &\approx (0.4433, 0.3981, 0.3529, 0.3365, 0.3077, 0.2913, 0.2678, 0.2297, 0.2227, 0.1960, 0.1229)^\top.
\end{aligned}$$

Thus we can take as an approximation

$$\mathbf{v} \approx (0.4433, 0.3981, 0.3529, 0.3365, 0.3077, 0.2913, 0.2678, 0.2297, 0.2227, 0.1960, 0.1229)^\top,$$

and the a-loadings are approximately given by

$$(a_\lambda)_{\lambda\in\mathcal{P}(n)} \approx (100.00, 85.89, 71.79, 66.66, 57.68, 52.55, 45.23, 33.32, 31.12, 22.81, 0.00).$$

In the above example of $n = 6$, we see that the a-loadings are compatible with the lexicographic order. In particular, the partition (6) has a-loading 100 and (1^6) has a-loading 0. However, in general, the a-loadings are *not completely* compatible with the lexicographic order though they are strongly correlated. For instance, when $n = 9$, the partition $(5, 1^4)$ has a-loading 55.32, while $(4, 4, 1)$ has 56.55. See Appendix A for the values of a-loadings. On the other hand, we say that $\lambda = (\lambda_1 \geq \lambda_2 \geq \cdots \geq \lambda_n)$ dominates $\mu = (\mu_1 \geq \mu_2 \geq \cdots \geq \mu_n)$ in the dominance order if $\lambda_1 + \cdots + \lambda_k \geq \mu_1 + \cdots \mu_k$ for all $k \geq 1$. Now one can observe that *the a-loadings are compatible with the dominance order.* [1]

Define a $p(n) \times p(n)$ symmetric matrix $\mathsf{Z}_n = [z_{\lambda,\mu}]_{\lambda,\mu\in\mathcal{P}(n)}$ by

$$z_{\lambda,\mu} = \|\lambda - \mu\|_1 \coloneqq \sum_{i=1}^n |\lambda_i - \mu_i|$$

for $\lambda = (\lambda_1, \lambda_2, \ldots, \lambda_n)$ and $\mu = (\mu_1, \mu_2, \ldots, \mu_n) \in \mathcal{P}(n)$. The matrix Z_n will be called the *difference* matrix of $\mathcal{P}(n)$.

[1] This was noticed by David Anderson after the first version of this paper was posted on the arXiv.

Example 2.7. When $n = 6$, we obtain

$$\mathsf{Z}_6 = \begin{bmatrix} 0 & 2 & 4 & 4 & 6 & 6 & 6 & 8 & 8 & 8 & 10 \\ 2 & 0 & 2 & 2 & 4 & 4 & 4 & 6 & 6 & 6 & 8 \\ 4 & 2 & 0 & 2 & 2 & 2 & 4 & 4 & 4 & 6 & 8 \\ 4 & 2 & 2 & 0 & 4 & 2 & 2 & 4 & 4 & 4 & 6 \\ 6 & 4 & 2 & 4 & 0 & 2 & 4 & 4 & 4 & 6 & 8 \\ 6 & 4 & 2 & 2 & 2 & 0 & 2 & 2 & 2 & 4 & 6 \\ 6 & 4 & 4 & 2 & 4 & 2 & 0 & 4 & 2 & 2 & 4 \\ 8 & 6 & 4 & 4 & 4 & 2 & 4 & 0 & 2 & 4 & 6 \\ 8 & 6 & 4 & 4 & 4 & 2 & 2 & 2 & 0 & 2 & 4 \\ 8 & 6 & 6 & 4 & 6 & 4 & 2 & 4 & 2 & 0 & 2 \\ 10 & 8 & 8 & 6 & 8 & 6 & 4 & 6 & 4 & 2 & 0 \end{bmatrix}.$$

Similarly to Y_n, all the eigenvalues of Z_n are real. It is easy to see that Z_n is irreducible, and hence the Perron–Frobenius theorem for matrices with nonnegative entries [10, Section III.2] tells us that Z_n has a unique eigenvalue of largest magnitude and that the corresponding eigenvector can be chosen to have strictly positive components.

Definition 2.8. Let $\mathbf{w} = (w_\lambda)_{\lambda \in \mathcal{P}(n)}$ be an eigenvector of the largest eigenvalue of Z_n such that $w_\lambda > 0$ for all $\lambda \in \mathcal{P}(n)$. Denote by $w_{\max}$ (resp. $w_{\min}$) a maximum (resp. minimum) of $\{w_\lambda\}_{\lambda \in \mathcal{P}(n)}$. Define

$$b_\lambda := 100 \times \frac{w_\lambda - w_{\min}}{w_{\max} - w_{\min}} \quad \text{for } \lambda \in \mathcal{P}(n).$$

The value b_λ is called the *b-loading* of partition $\lambda \in \mathcal{P}(n)$.

Like Definition 2.5, the above definition introduces a new concept into the study of Kronecker coefficients. We will show its usefulness in Section 4. The power iteration works equally well to compute $\mathbf{w}$: Let $\mathbf{w}_0 = (1, 0, \dots, 0)^\top$ and define

$$\mathbf{w}_{k+1} = \frac{\mathsf{Z}_n \mathbf{w}_k}{\|\mathsf{Z}_n \mathbf{w}_k\|_2}.$$

Then the limit

$$\mathbf{w} = \lim_{k \to \infty} \mathbf{w}_k$$

is an eigenvector of the largest eigenvalue of Z_n.

Example 2.9. When $n = 6$, we have

$$\begin{aligned} \mathbf{w}_1 &\approx (0.0000, 0.0958, 0.1916, 0.1916, 0.2873, 0.2873, 0.2873, 0.3831, 0.3831, 0.3831, 0.4789)^\top, \\ \mathbf{w}_2 &\approx (0.5177, 0.3705, 0.2992, 0.2565, 0.3087, 0.2042, 0.2042, 0.2517, 0.1947, 0.2280, 0.3277)^\top, \\ &\vdots \\ \mathbf{w}_{10} &\approx (0.4046, 0.2962, 0.2662, 0.2394, 0.3061, 0.2318, 0.2393, 0.3060, 0.2662, 0.2961, 0.4044)^\top, \\ \mathbf{w}_{11} &\approx (0.4045, 0.2961, 0.2662, 0.2393, 0.3061, 0.2318, 0.2393, 0.3061, 0.2662, 0.2962, 0.4045)^\top, \\ \mathbf{w}_{12} &\approx (0.4045, 0.2961, 0.2662, 0.2393, 0.3061, 0.2318, 0.2393, 0.3061, 0.2662, 0.2961, 0.4045)^\top. \end{aligned}$$

Thus we can take as an approximation

$$\mathbf{w} \approx (0.4045, 0.2961, 0.2662, 0.2393, 0.3061, 0.2318, 0.2393, 0.3061, 0.2662, 0.2961, 0.4045)^\top,$$

and the b-loadings are approximately given by

$$(b_\lambda)_{\lambda \in \mathcal{P}(n)} \approx (100.00, 37.25, 19.93, 4.36, 43.01, 0.00, 4.36, 43.01, 19.93, 37.25, 100.00).$$

Remark 2.10. In the above example, we notice that the partitions (6) and (1^6) both have b-loading 100 and the partition $(3, 2, 1)$ has b-loading 0. In general, we observe that *if λ and μ are conjugate in $\mathcal{P}(n)$, then their b-loadings are the same, i.e., $b_\lambda = b_\mu$.*

Remark 2.11. It would be interesting to combinatorially characterize the loadings of $\lambda \in \mathcal{P}(n)$.

For $\mathbf{t} = (\lambda, \mu, \nu) \in \mathcal{P}(n)^3$, we will write

$$g(\mathbf{t}) := g^{\nu}_{\lambda,\mu}.$$

Definition 2.12. Let $\mathbf{t} = (\lambda, \mu, \nu) \in \mathcal{P}(n)^3$. Define the *a-loading* (resp. *b-loading*) of $\mathbf{t}$, denoted by $a(\mathbf{t})$ (resp. $b(\mathbf{t})$), to be the sum of the a-loadings (resp. b-loadings) of λ, μ, and ν, i.e.,

$$a(\mathbf{t}) := a_\lambda + a_\mu + a_\nu \qquad (\text{resp. } b(\mathbf{t}) := b_\lambda + b_\mu + b_\nu).$$

2.1. Connections to PCA and kernel methods

The definitions of similitude and difference matrices are closely related to PCA and kernel methods (see, e.g., [11, Sections 3.5 and 12.3]), respectively. Indeed, we look at the matrix $\mathsf{P}_n^\top$ as a data matrix.

Example 2.13. When $n = 6$, we get

$$\mathsf{P}_6^\top = \begin{bmatrix} 6 & 5 & 4 & 4 & 3 & 3 & 3 & 2 & 2 & 2 & 1 \\ 0 & 1 & 2 & 1 & 3 & 2 & 1 & 2 & 2 & 1 & 1 \\ 0 & 0 & 0 & 1 & 0 & 1 & 1 & 2 & 1 & 1 & 1 \\ 0 & 0 & 0 & 0 & 0 & 0 & 1 & 0 & 1 & 1 & 1 \\ 0 & 0 & 0 & 0 & 0 & 0 & 0 & 0 & 0 & 1 & 1 \\ 0 & 0 & 0 & 0 & 0 & 0 & 0 & 0 & 0 & 0 & 1 \end{bmatrix},$$

and consider this as a data matrix of 6 data points with 11 features.

Since the average of each column is 1 for $\mathsf{P}_n^\top$, the covariance matrix of the data matrix $\mathsf{P}_n^\top$ is $(\mathsf{P}_n - \mathbb{1})(\mathsf{P}_n - \mathbb{1})^\top$, where $\mathbb{1}$ is the matrix with all entries equal to 1. As there are no significant differences in the largest eigenvalues or the directions of their eigenvectors, we use the similitude matrix $\mathsf{Y}_n = \mathsf{P}_n\mathsf{P}_n^\top$ as a substitute for the covariance matrix. Then an eigenvector of the largest eigenvalue of Y_n provides a good approximation to a weight vector of the first principal component, leading to the definition of a-loadings.

The idea of a kernel method is to embed a dataset into a different space of (usually) higher dimension. In order to utilize this idea, we consider the matrix P_n as a data matrix with $p(n)$ data points and n features. Then we map a partition λ, which is an n-dimensional row vector of P_n, onto the $p(n)$-dimensional vector $(\|\lambda - \mu\|_1)_{\mu \in \mathcal{P}(n)}$, and the resulting new matrix is exactly the difference matrix Z_n.

Example 2.14. When $n = 6$, we obtain

$$\mathsf{P}_6 = \begin{bmatrix} 6 & 0 & 0 & 0 & 0 & 0 \\ 5 & 1 & 0 & 0 & 0 & 0 \\ 4 & 2 & 0 & 0 & 0 & 0 \\ 4 & 1 & 1 & 0 & 0 & 0 \\ 3 & 3 & 0 & 0 & 0 & 0 \\ 3 & 2 & 1 & 0 & 0 & 0 \\ 3 & 1 & 1 & 1 & 0 & 0 \\ 2 & 2 & 2 & 0 & 0 & 0 \\ 2 & 2 & 1 & 1 & 0 & 0 \\ 2 & 1 & 1 & 1 & 1 & 0 \\ 1 & 1 & 1 & 1 & 1 & 1 \end{bmatrix} \quad \mapsto \quad \mathsf{Z}_6 = \begin{bmatrix} 0 & 2 & 4 & 4 & 6 & 6 & 6 & 8 & 8 & 8 & 10 \\ 2 & 0 & 2 & 2 & 4 & 4 & 4 & 6 & 6 & 6 & 8 \\ 4 & 2 & 0 & 2 & 2 & 2 & 4 & 4 & 4 & 6 & 8 \\ 4 & 2 & 2 & 0 & 4 & 2 & 2 & 4 & 4 & 4 & 6 \\ 6 & 4 & 2 & 4 & 0 & 2 & 4 & 4 & 4 & 6 & 8 \\ 6 & 4 & 2 & 2 & 2 & 0 & 2 & 2 & 2 & 4 & 6 \\ 6 & 4 & 4 & 2 & 4 & 2 & 0 & 4 & 2 & 2 & 4 \\ 8 & 6 & 4 & 4 & 4 & 2 & 4 & 0 & 2 & 4 & 6 \\ 8 & 6 & 4 & 4 & 4 & 2 & 2 & 2 & 0 & 2 & 4 \\ 8 & 6 & 6 & 4 & 6 & 4 & 2 & 4 & 2 & 0 & 2 \\ 10 & 8 & 8 & 6 & 8 & 6 & 4 & 6 & 4 & 2 & 0 \end{bmatrix}.$$

Since the difference matrix Z_n is a symmetric matrix, we consider an eigenvector of the largest eigenvalue of Z_n to obtain the direction of largest variations in the differences. This leads to the definition of b-loadings.

3. Distributions of loadings

In this section, we present the histograms of loadings and describe the corresponding distributions. First, we consider all the triples of $\mathbf{t} \in \mathcal{P}(n)^3$, and after that, separate them according to whether $g(\mathbf{t}) \neq 0$ or $= 0$. All the histograms in this section have a bin size of 100.

Figure 1 (resp. Figure 2) has the histograms of a-loadings (resp. b-loadings) of $\mathbf{t} \in \mathcal{P}(n)^3$ for $n = 14, 15, 16$. According to what the histograms suggest, we propose a conjecture:

Conjecture 3.1. *Consider $\mathcal{P}(n)^3$ as a sample space. Then the sequence of random variables X_n^a (resp. X_n^b) defined by the a-loadings (resp. b-loadings) of* $\mathbf{t}$ *converges in distribution to a normal (resp. gamma) random variable as $n \to \infty$.*

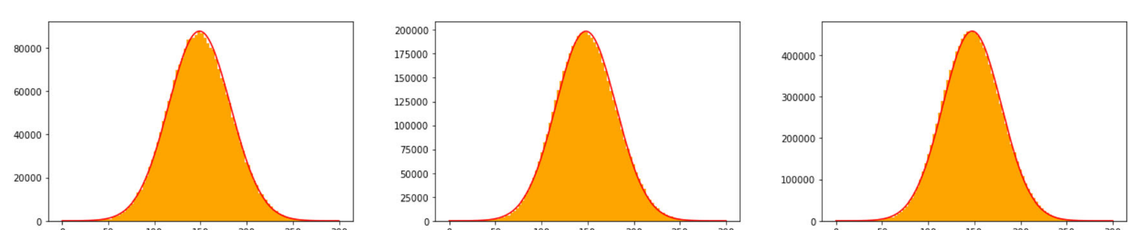

Figure 1. Histograms of a-loadings of $\mathbf{t} \in \mathcal{P}(n)^3$ for $n = 14, 15, 16$ from left to right along with curves (red) of normal distributions.

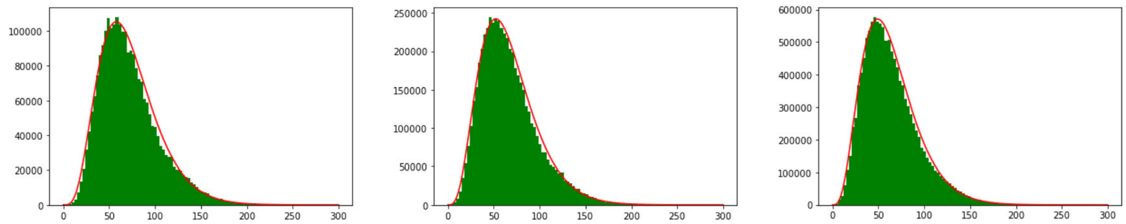

Figure 2. Histograms of b-loadings of $\mathbf{t} \in \mathcal{P}(n)^3$ for $n = 14, 15, 16$ from left to right along with curves (red) of gamma distributions.

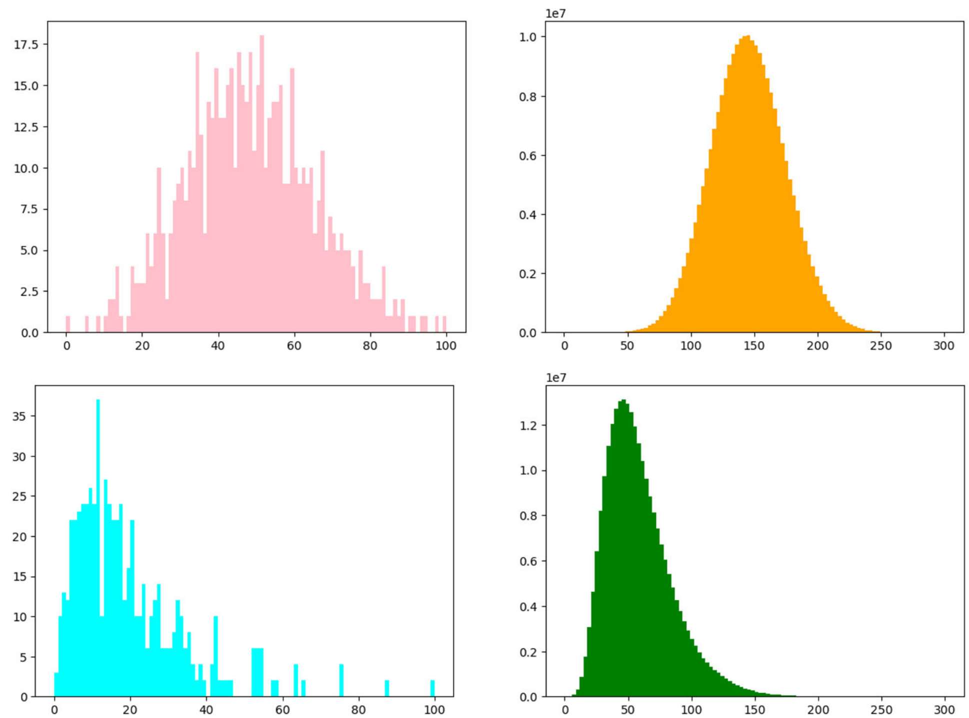

Figure 3. Histograms of a-loadings of $\lambda \in \mathcal{P}(n)$ (top-left) and $\mathbf{t} \in \mathcal{P}(n)^3$ (top-right) and histograms of b-loadings of λ (bottom-left) and $\mathbf{t}$ (bottom-right) when $n = 20$.

We sketch the curves of normal distributions on the histograms in Figure 1. Here we note that the mean is not exactly 150. Actually, the mean values of the a-loadings are approximately 148.86, 148.15, 147.65 for $n = 14, 15, 16$, respectively. Similarly, we draw the curves of gamma distributions in Figure 2. The mean values of the b-loadings are approximately 72.07, 66.71, 63.48 for $n = 14, 15, 16$, respectively. When $n = 14, 15, 16$, the histograms of the loadings of partitions $\lambda \in \mathcal{P}(n)$, in contrast to triples $\mathbf{t} \in \mathcal{P}(n)^3$, lack sufficient data points to ascertain their underlying distributions. (Note that $p(16) = 231$.) Nonetheless, since a_λ, a_μ and a_ν are computed independently for $a(\mathbf{t}) = a_\lambda + a_\mu + a_\nu$, and the sum of normal random variables is itself normal, it seems reasonable to expect that the a-loadings of λ follow a normal distribution. By the same reasoning, we conjecture that the b-loadings of λ follow a gamma distribution. If the conjectures are true, the loadings of $\mathbf{t} \in \mathcal{P}(n)^3$ will naturally have the distribution given as a sum of three independent distributions. (Recall Definition 2.12.) Figure 3 has the histograms of loadings of λ and $\mathbf{t}$ when $n = 20$, which seem to be consistent with this expectation.

4. Separation of $g(\mathbf{t}) \neq 0$ from $g(\mathbf{t}) = 0$

In this section, we consider the distributions of loadings according to whether the Kronecker coefficients $g(\mathbf{t})$ are zero or nonzero. Using minimum values of loadings in each case, we will obtain vertical lines which separate the distributions of these two cases.

In Figures 4–7, we present the ranges and histograms of loadings of $\mathbf{t} \in \mathcal{P}(n)^3$ for $n = 10, 11, 12, 13$ according to whether $g(\mathbf{t}) \neq 0$ (red) or $= 0$ (blue). In Figure 4, the y-values 0 and 1 represent the cases $g(\mathbf{t}) = 0$ and $g(\mathbf{t}) \neq 0$, respectively, while the x-value is the a-loading of $\mathbf{t}$. The same convention applies to Figure 6 with b-loadings. As one can see, the ranges and histograms do not vary much as n varies. The separation between the regions corresponding to $g(\mathbf{t}) \neq 0$ (red) and $= 0$ (blue) is more distinctive in the case of b-loadings. It is clear that we may use the minimum values of loadings to obtain vertical lines that separate the red regions from the blue ones.

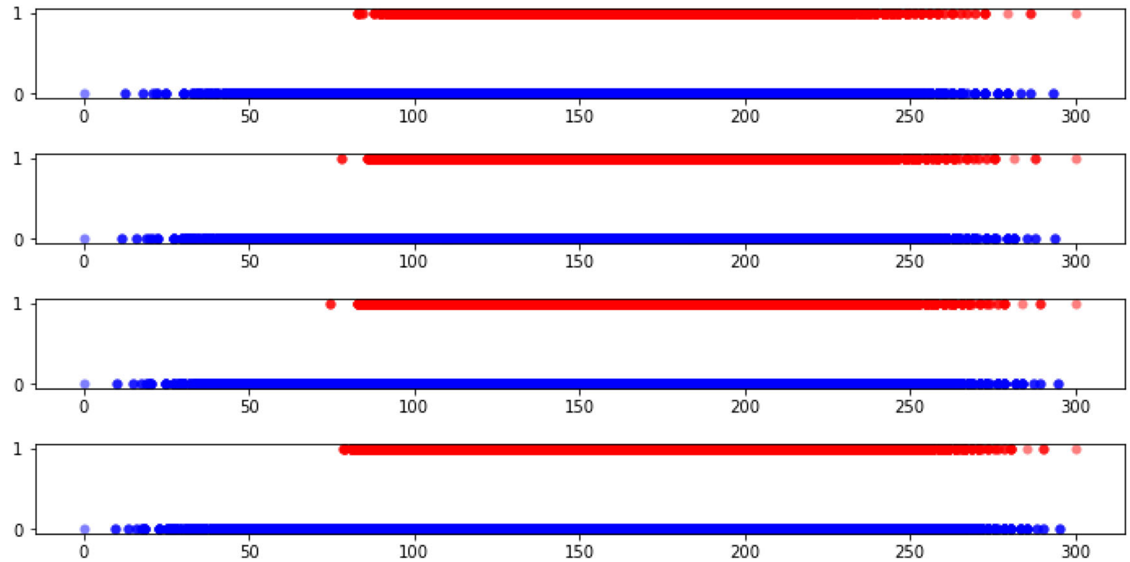

Figure 4. Ranges of a-loadings for $n = 10, 11, 12, 13$ from top to bottom. A red (resp. blue) dot at $(x, 1)$ (resp. $(x, 0)$) corresponds to $\mathbf{t} \in \mathcal{P}(n)^3$ with $a(\mathbf{t}) = x$ and $g(\mathbf{t}) \neq 0$ (resp. $g(\mathbf{t}) = 0$).

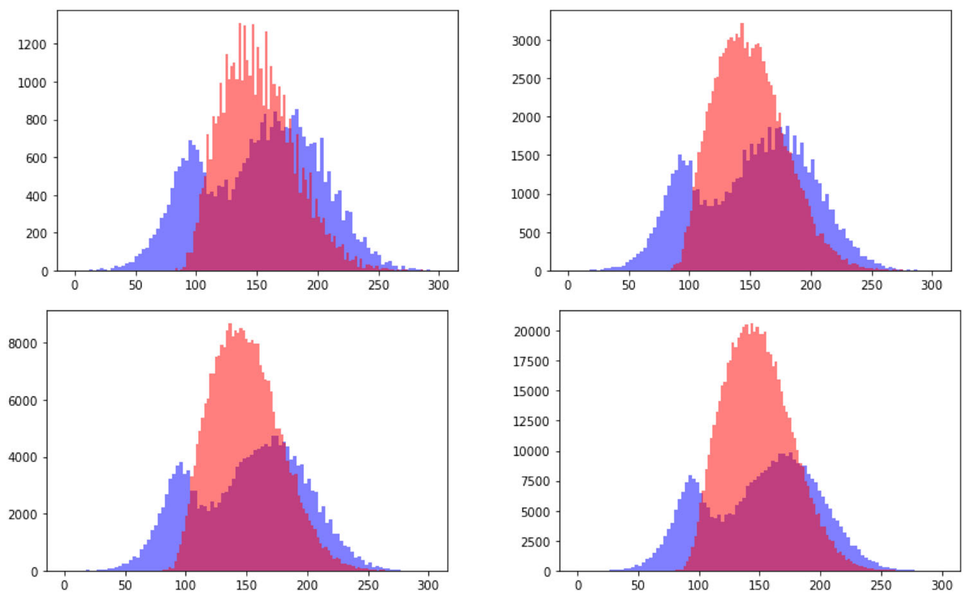

Figure 5. Histograms of a-loadings for $n = 10$ (top-left), 11 (top-right), 12 (bottom-left), and 13 (bottom-right). The red (resp. blue) region represents the numbers of $\mathbf{t}$ such that $g(\mathbf{t}) \neq 0$ (resp. $g(\mathbf{t}) = 0$).

With this in mind, define

$$a_\star := \min\{a(\mathbf{t}) : g(\mathbf{t}) \neq 0, \mathbf{t} \in \mathcal{P}(n)^3\},$$
$$b_\star := \min\{b(\mathbf{t}) : g(\mathbf{t}) = 0, \mathbf{t} \in \mathcal{P}(n)^3\}.$$

Then, for $\mathbf{t} \in \mathcal{P}(n)^3$,

$$\text{if } a(\mathbf{t}) < a_\star \text{ then } g(\mathbf{t}) = 0 \ \text{ and } \ \boxed{\text{if } b(\mathbf{t}) < b_\star \text{ then } g(\mathbf{t}) \neq 0}. \tag{4.1}$$

This provides sufficient conditions for $g(\mathbf{t}) = 0$ and $g(\mathbf{t}) \neq 0$, respectively, once we know the values of $a_\star$ and $b_\star$.

In this way, the values of $b_\star$ can be used quite effectively in distinguishing $g(\mathbf{t}) \neq 0$ from $g(\mathbf{t}) = 0$. When $n = 20$, the percentage of $\mathbf{t}$ satisfying $b(\mathbf{t}) < b_\star$ is about 31.8%. In contrast, the values $a_\star$ do not turn out to be very useful for bigger n in distinguishing $g(\mathbf{t}) = 0$ from $g(\mathbf{t}) \neq 0$. When $n = 20$, the percentage of $\mathbf{t}$ satisfying $a(\mathbf{t}) < a_\star$ is only 0.37%. See Example 4.1 (2) below for more details. Nonetheless, the values of $a_\star$ are interesting in their own right and can be valuable for analyzing the distribution of the a-loadings in relation to the Kronecker coefficients.

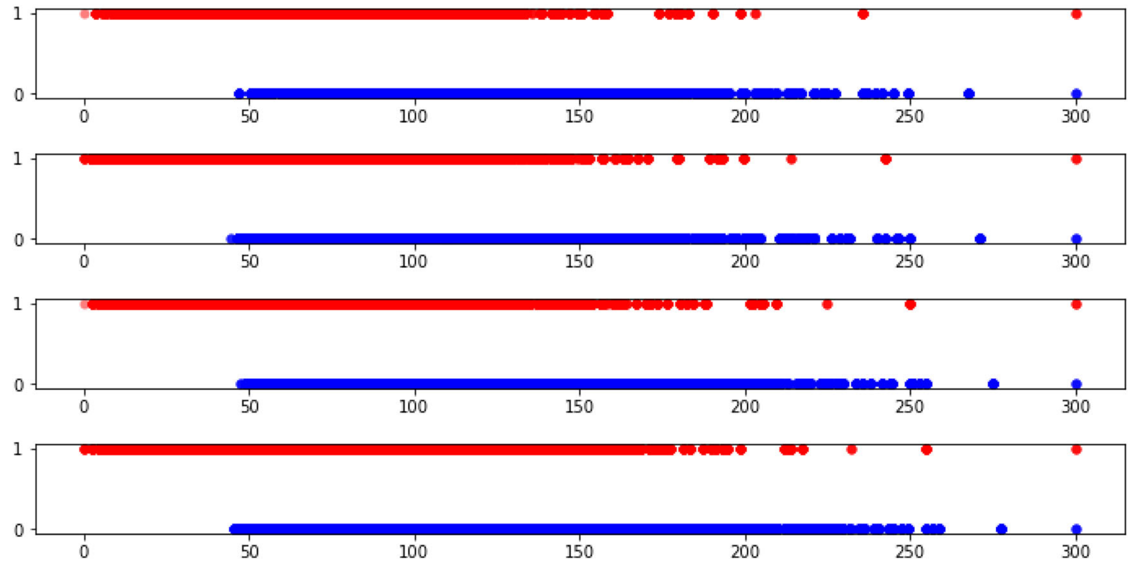

Figure 6. Ranges of b-loadings for $n = 10, 11, 12, 13$ from top to bottom. A red (resp. blue) dot at $(x, 1)$ (resp. $(x, 0)$) corresponds to $\mathbf{t} \in \mathcal{P}(n)^3$ with $b(\mathbf{t}) = x$ and $g(\mathbf{t}) \neq 0$ (resp. $g(\mathbf{t}) = 0$).

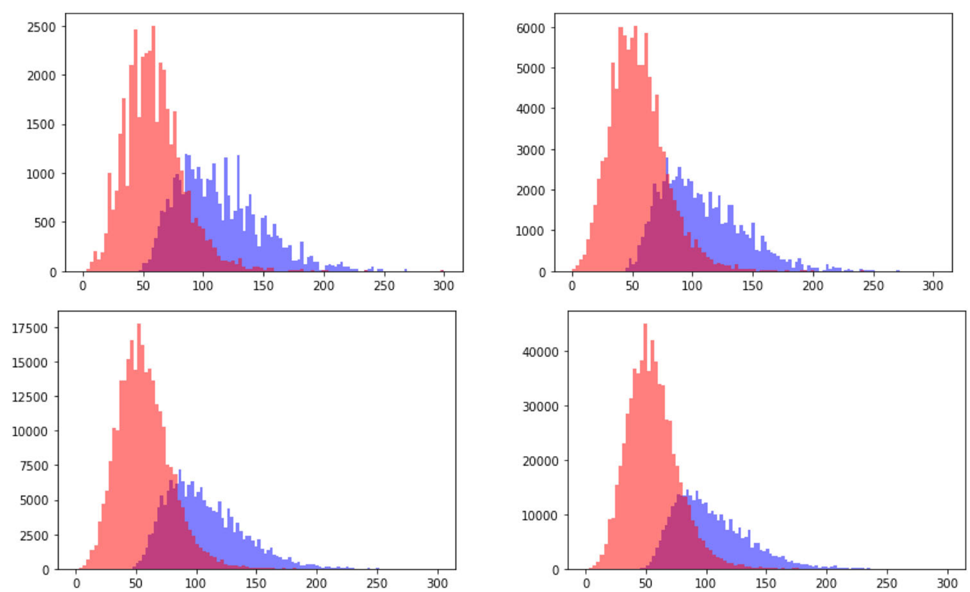

Figure 7. Histograms of b-loadings for $n = 10$ (top-left), 11 (top-right), 12 (bottom-left) and 13 (bottom-right). The red (resp. blue) region represents the numbers of $\mathbf{t}$ such that $g(\mathbf{t}) \neq 0$ (resp. $g(\mathbf{t}) = 0$).

Example 4.1.

1. When $n = 18$, we obtain $b_\star \approx 44.18$. Now that the b-loading of

$$\mathbf{t} = ((12, 4, 2), (8, 4, 2, 2, 1, 1), (5, 4, 3, 3, 1, 1, 1))$$

is readily computed to be approximately $41.07 < b_\star$, we immediately conclude that $g(\mathbf{t}) \neq 0$ by (4.1).
2. When $n = 20$, there are 246, 491, 883 triples $\mathbf{t} \in \mathcal{P}(20)$. Among them, 78, 382, 890 triples satisfy $b(\mathbf{t}) < b_\star \approx 43.74$ so that $g(\mathbf{t}) \neq 0$. The percentage of these triples is about 31.8%. On the other hand, 909, 200 triples satisfy $a(\mathbf{t}) < a_\star \approx 70.88$ and the percentage is only 0.37%.

Remark 4.2. It appears that the b-loadings of $\mathbf{t}$ with $g(\mathbf{t}) \neq 0$ is a gamma distribution by itself. See the histogram and the curve of a gamma distribution when $n = 13$ in Figure 8.

In the rest of this section, computational results of the values of $a_\star$ and $b_\star$ for $6 \leq n \leq 20$ will be presented along with some conjectures.

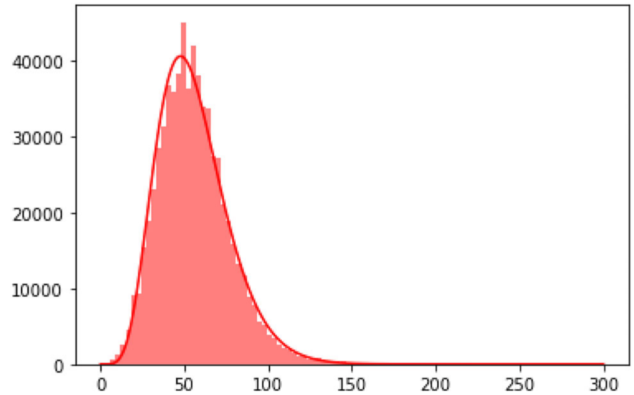

Figure 8. Histogram and curve (red) of a gamma distribution when $n = 13$.

Table 1. Values of $a_\star$ and $\mathbf{t} = (\lambda, \mu, \nu)$ such that $a_\star = a(\mathbf{t})$ and $\lambda \geq \mu \geq \nu$ lexicographically.

n	$a_\star$	λ	μ	ν
6	90.9986	$(3,3)$	$(2,2,2)$	(1^6)
7	85.0932	$(2,2,2,1)$	$(2,2,2,1)$	$(2,2,2,1)$
8	79.1637	(2^4)	(2^4)	(2^4)
9	84.5605	$(3,2,2,2)$	$(2^4,1)$	$(2^4,1)$
10	82.5959	$(3,3,2,2)$	(2^5)	$(2^4,1)$
11	78.1018	$(3,3,3,2)$	$(2^5,1)$	$(2^5,1)$
12	74.6018	(3^4)	(2^6)	(2^6)
13	78.1813	$(4,3,3,3)$	$(2^6,1)$	$(2^6,1)$
14	77.3651	$(4,4,3,3)$	(2^7)	$(2^6,1,1)$
15	74.8437	$(4,4,4,3)$	$(2^7,1)$	$(2^7,1)$
16	72.1837	(4^4)	(2^8)	(2^8)
17	71.2716	$(3^5,2)$	$(3^5,2)$	$(2^8,1)$
18	68.9559	(3^6)	(3^6)	(2^9)
19	71.9678	$(4,3^5)$	$(3^6,1)$	$(2^9,1)$
20	70.8806	(5^4)	(2^{10})	(2^{10})

When $n = 8, 12, 16, 20$, the partitions λ, μ, ν are highlighted in blue to emphasize a pattern leading to Conjecture 4.3.

Table 2. Under Conjecture 4.3, values of $a_\star$ and $\mathbf{t} = ((k^4), (2^{2k}), (2^{2k}))$ for $n = 4k$ such that $a_\star = a(\mathbf{t})$.

n	$a_\star$	$\mathbf{t}$
24	70.0772	$((6^4), (2^{12}), (2^{12}))$
28	69.5351	$((7^4), (2^{14}), (2^{14}))$
32	69.1732	$((8^4), (2^{16}), (2^{16}))$
36	68.9254	$((9^4), (2^{18}), (2^{18}))$
40	68.7518	$((10^4), (2^{20}), (2^{20}))$
44	68.6334	$((11^4), (2^{22}), (2^{22}))$
48	68.5549	$((12^4), (2^{24}), (2^{24}))$

4.1. *Results on a-loadings*

We compute and record $a_\star$ and $\mathbf{t} = (\lambda, \mu, \nu)$ such that $a_\star = a(\mathbf{t})$ and $\lambda \geq \mu \geq \nu$ lexicographically, for $6 \leq n \leq 20$ in Table 1. We do not consider $n \leq 5$ because they seem to be too small for statistical analysis.

Based on the results of $n = 8, 12, 16, 20$ as written in blue in Table 1, we make the following conjecture.

Conjecture 4.3. Recall $a_\star := \min\{a(\mathbf{t}) : g(\mathbf{t}) \neq 0, \mathbf{t} \in \mathcal{P}(n)^3\}$, where $a(\mathbf{t}) := a_\lambda + a_\mu + a_\nu$ and $g(\mathbf{t}) := g^{\nu}_{\lambda,\mu}$ for $\mathbf{t} = (\lambda, \mu, \nu) \in \mathcal{P}(n)^3$. When $n = 4k$ $(k \geq 2)$, the values $a_\star$ are attained by $\mathbf{t} = ((k^4), (2^{2k}), (2^{2k}))$.

As an exhaustive computation for all possible triples becomes exponentially expensive, we assume that Conjecture 4.3 is true and continue computation. The results are in Table 2. Since we know $\mathbf{t}$ exactly under Conjecture 4.3, we could calculate $a_\star$ for n much bigger than those n in the case of $b_\star$ that will be presented in Table 4.

Remark 4.4. The values of $a_\star$ seem to keep decreasing though slowly. However, it is not clear whether $a_\star$ converges to a limit as $n \to \infty$.

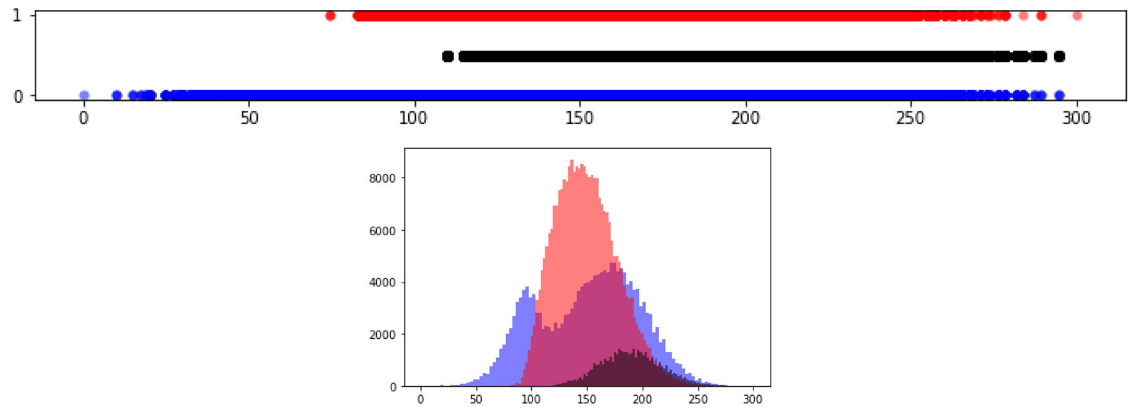

Figure 9. Ranges of a-loadings where a black dot at $(x, \frac{1}{2})$ corresponds to $\mathbf{t} \in \mathcal{P}(12)^3$ satisfying the condition in (4.2) with $a(\mathbf{t}) = x$ and $g(\mathbf{t}) = 0$ and histograms of a-loadings where the dark brown region represents the numbers of $\mathbf{t}$ satisfying the condition in (4.2) and $g(\mathbf{t}) = 0$.

Table 3. Values of $b_\star$ and $\mathbf{t} = (\lambda, \mu, \nu)$ such that $b_\star = b(\mathbf{t})$.

n	$b_\star$	λ	μ	ν
6	59.7812	$(2, 2, 1, 1)$	$(2, 2, 1, 1)$	$(2, 2, 1, 1)$
7	47.9477	$(3, 3, 1)$	$(3, 1^4)$	$(3, 1^4)$
8	54.6650	$(3, 2, 1, 1, 1)$	$(3, 2, 1, 1, 1)$	$(2, 2, 1^4)$
9	39.8213	$(3, 2, 1^4)$	$(3, 2, 1^4)$	$(3, 2, 1^4)$
10	46.6592	$(4, 2, 1^4)$	$(3, 2, 1^5)$	$(3, 2, 1^5)$
11	44.4953	$(6, 1^5)$	$(6, 1^5)$	$(4, 3, 3, 1)$
12	47.3571	$(3, 3, 2, 1^4)$	$(3, 3, 2, 1^4)$	$(3, 3, 2, 1^4)$
13	45.1104	$(4, 3, 2, 1^4)$	$(3, 3, 2, 1^5)$	$(3, 3, 2, 1^5)$
14	44.9312	$(4, 3, 2, 1^5)$	$(4, 3, 2, 1^5)$	$(3, 3, 2, 1^6)$
15	40.3916	$(4, 3, 2, 1^6)$	$(4, 3, 2, 1^6)$	$(4, 3, 2, 1^6)$
16	41.7064	$(5, 3, 2, 1^6)$	$(4, 3, 2, 1^7)$	$(4, 3, 2, 1^7)$
17	43.4181	$(5, 3, 2, 1^7)$	$(4, 3, 2, 2, 1^6)$	$(4, 3, 2, 2, 1^6)$
18	44.1817	$(4, 4, 2, 2, 1^6)$	$(4, 4, 2, 2, 1^6)$	$(4, 4, 2, 2, 1^6)$
19	44.3797	$(5, 4, 2, 2, 1^6)$	$(4, 4, 2, 2, 1^7)$	$(4, 4, 2, 2, 1^7)$
20	43.7424	$(5, 4, 2, 2, 1^7)$	$(4, 4, 3, 2, 1^7)$	$(4, 4, 3, 2, 1^7)$

When $n = 6, 9, 12, 15, 18$, the partitions λ, μ, ν are highlighted in blue to emphasize the pattern $\lambda = \mu = \nu$ leading to Conjecture 4.6.

Notice that we have a sufficient condition for $g(\mathbf{t}) = 0$ by taking the contrapositive of (2.1):

$$d_\nu < |d_\lambda - d_\mu| \quad \text{or} \quad d_\nu > d_\lambda + d_\mu \quad \Longrightarrow \quad g(\mathbf{t}) = 0. \tag{4.2}$$

As $a_\star$ provides another sufficient condition for $g(\mathbf{t}) = 0$ in (4.1), one may be curious about their relationship. As a matter of fact, we observe that

$$a_\star < a(\mathbf{t}) \qquad \text{for any } \mathbf{t} \text{ satisfying the condition in (4.2).}$$

Thus conditions in (4.1) and (4.2) for $g(\mathbf{t}) = 0$ do not have overlaps. Let us look at pictures when $n = 12$. In the top graph of Figure 9, red dots and blue dots are the same as in Figure 4, while a black dot at $(x, \frac{1}{2})$ corresponds to $\mathbf{t} \in \mathcal{P}(12)^3$ satisfying the condition in (4.2) with $a(\mathbf{t}) = x$ and $g(\mathbf{t}) = 0$. In the bottom histograms of Figure 9, the red region and blue region are the same as in Figure 5, while the dark brown region represents the numbers of $\mathbf{t}$ satisfying the condition in (4.2) and $g(\mathbf{t}) = 0$.

4.2. *Results on b-loadings*

In Table 3, we list $b_\star$ and $\mathbf{t} = (\lambda, \mu, \nu)$ such that $b_\star = b(\mathbf{t})$ and $\lambda \geq \mu \geq \nu$ in lexicographic order for $6 \leq n \leq 20$. When there are more than one $\mathbf{t}$ such that $b_\star = b(\mathbf{t})$, we only record the lexicographically smallest one. (Recall Remark 2.10.)

Example 4.5. When $n = 16$, we get $b_\star = b(\mathbf{t}_1) = b(\mathbf{t}_2) = b(\mathbf{t}_3)$ with

$$\begin{aligned} \mathbf{t}_1 &= [(10, 3, 2, 1), (10, 3, 2, 1), (5, 3, 2, 1^6)], \\ \mathbf{t}_2 &= [(10, 3, 2, 1), (9, 3, 2, 1, 1), (4, 3, 2, 1^7)], \\ \mathbf{t}_3 &= [(5, 3, 2, 1^6), (4, 3, 2, 1^7), (4, 3, 2, 1^7)], \end{aligned}$$

and only $\mathbf{t}_3$ is recorded in the table.

Table 4. Under Conjecture 4.6, values of $b_\star$ and $\mathbf{t} = (\lambda, \lambda, \lambda)$ for $n = 3k$ such that $b_\star = b(\mathbf{t})$.

n	$b_\star$	$\lambda = \mu = \nu$
21	45.0545	$(5, 4, 2, 2, 1^8)$
24	43.7126	$(5, 4, 3, 2, 2, 1^8)$
27	44.0699	$(5, 5, 3, 3, 2, 1^9)$
30	45.0141	$(5, 5, 4, 3, 2, 2, 1^9)$
33	44.7615	$(6, 6, 4, 3, 2, 1^{12})$
36	44.3350	$(6, 6, 4, 3, 2^3, 1^{11})$

Drawing from the results in Table 3—particularly those for $n = 6, 9, 12, 15, 18$ highlighted in blue—we propose the following conjecture.

Conjecture 4.6. Recall $b_\star \coloneqq \min\{b(\mathbf{t}) : g(\mathbf{t}) = 0, \mathbf{t} \in \mathcal{P}(n)^3\}$, where $b(\mathbf{t}) \coloneqq b_\lambda + b_\mu + b_\nu$ and $g(\mathbf{t}) \coloneqq g^{\nu}_{\lambda,\mu}$ for $\mathbf{t} = (\lambda, \mu, \nu) \in \mathcal{P}(n)^3$. For $n \geq 6$, the values $b_\star$ are attained by $\mathbf{t} = (\lambda, \mu, \nu)$ such that $\lambda = \mu$ or $\mu = \nu$. Moreover, when $n = 3k$, $k \geq 2$, the values $b_\star$ are attained by $\mathbf{t} = (\lambda, \mu, \nu)$ such that $\lambda = \mu = \nu$.

Analogous to the case of $a_\star$, we assume Conjecture 4.6 holds for $n = 3k$ and proceed with the computation. The results are presented in Table 4.

Remark 4.7. The values of $b_\star$ appear to fluctuate with diminishing amplitudes as n increases. However, it remains unclear whether $b_\star$ converges as $n \to \infty$.

Appendix A: Table of loadings

We tabulate the a-loading a_λ and b-loading b_λ of each partition $\lambda \in \mathcal{P}(n)$ for $6 \leq n \leq 12$.

λ	a_λ	b_λ
$(6,0,0,0,0,0)$	100.0	100.0
$(5,1,0,0,0,0)$	85.8934	37.252
$(4,2,0,0,0,0)$	71.7868	19.9271
$(4,1,1,0,0,0)$	66.6591	4.363
$(3,3,0,0,0,0)$	57.6803	43.005
$(3,2,1,0,0,0)$	52.5526	0.0
$(3,1,1,1,0,0)$	45.2311	4.363
$(2,2,2,0,0,0)$	33.3183	43.005
$(2,2,1,1,0,0)$	31.1245	19.9271
$(2,1,1,1,1,0)$	22.8133	37.252
$(1,1,1,1,1,1)$	0.0	100.0
$(7,0,0,0,0,0,0)$	100.0	100.0
$(6,1,0,0,0,0,0)$	88.302	47.507
$(5,2,0,0,0,0,0)$	76.604	26.483
$(5,1,1,0,0,0,0)$	72.8338	13.1061
$(4,3,0,0,0,0,0)$	64.906	36.928
$(4,2,1,0,0,0,0)$	61.1358	0.0
$(4,1,1,1,0,0,0)$	55.5306	1.81
$(3,3,1,0,0,0,0)$	49.4378	21.735
$(3,2,2,0,0,0,0)$	45.6676	21.735
$(3,2,1,1,0,0,0)$	43.8326	0.0
$(3,1,1,1,1,0,0)$	37.3978	13.1061
$(2,2,2,1,0,0,0)$	28.3644	36.928
$(2,2,1,1,1,0,0)$	25.6998	26.483
$(2,1,1,1,1,1,0)$	18.7933	47.507
$(1,1,1,1,1,1,1)$	0.0	100.0
$(8,0,0,0,0,0,0,0)$	100.0	100.0
$(7,1,0,0,0,0,0,0)$	90.5921	58.055
$(6,2,0,0,0,0,0,0)$	81.1842	35.198
$(6,1,1,0,0,0,0,0)$	77.6539	28.246
$(5,3,0,0,0,0,0,0)$	71.7763	34.854
$(5,2,1,0,0,0,0,0)$	68.2461	9.7331
$(5,1,1,1,0,0,0,0)$	63.194	12.637
$(4,4,0,0,0,0,0,0)$	62.3685	48.552
$(4,3,1,0,0,0,0,0)$	58.8382	15.265
$(4,2,2,0,0,0,0,0)$	55.3079	15.265
$(4,2,1,1,0,0,0,0)$	53.7861	0.0
$(4,1,1,1,1,0,0,0)$	47.8449	12.637
$(3,3,2,0,0,0,0,0)$	45.9	30.531
$(3,3,1,1,0,0,0,0)$	44.3782	15.265
$(3,2,2,1,0,0,0,0)$	40.8479	15.265
$(3,2,1,1,1,0,0,0)$	38.437	9.7331
$(3,1,1,1,1,1,0,0)$	32.0837	28.246
$(2,2,2,2,0,0,0,0)$	26.3879	48.552
$(2,2,2,1,1,0,0,0)$	25.4988	34.854
$(2,2,1,1,1,1,0,0)$	22.6758	35.198
$(2,1,1,1,1,1,1,0)$	16.0886	58.055
$(1,1,1,1,1,1,1,1)$	0.0	100.0
$(9,0,0,0,0,0,0,0,0)$	100.0	100.0
$(8,1,0,0,0,0,0,0,0)$	91.876	62.802
$(7,2,0,0,0,0,0,0,0)$	83.7521	39.559
$(7,1,1,0,0,0,0,0,0)$	80.9205	33.587
$(6,3,0,0,0,0,0,0,0)$	75.6281	34.591
$(6,2,1,0,0,0,0,0,0)$	72.7965	13.273
$(6,1,1,1,0,0,0,0,0)$	68.4825	16.425
$(5,4,0,0,0,0,0,0,0)$	67.5041	42.455
$(5,3,1,0,0,0,0,0,0)$	64.6726	12.1941
$(5,2,2,0,0,0,0,0,0)$	61.841	12.1941

λ	a_λ	b_λ
$(5,2,1,1,0,0,0,0,0)$	60.3586	0.0
$(5,1,1,1,1,0,0,0,0)$	55.3152	10.278
$(4,4,1,0,0,0,0,0,0)$	56.5486	26.205
$(4,3,2,0,0,0,0,0,0)$	53.7171	17.261
$(4,3,1,1,0,0,0,0,0)$	52.2346	5.067
$(4,2,2,1,0,0,0,0,0)$	49.4031	5.067
$(4,2,1,1,1,0,0,0,0)$	47.1912	0.0
$(4,1,1,1,1,1,0,0,0)$	41.7289	16.425
$(3,3,3,0,0,0,0,0,0)$	42.7616	39.778
$(3,3,2,1,0,0,0,0,0)$	41.2791	17.261
$(3,3,1,1,1,0,0,0,0)$	39.0672	12.1941
$(3,2,2,2,0,0,0,0,0)$	36.9651	26.205
$(3,2,2,1,1,0,0,0,0)$	36.2357	12.1941
$(3,2,1,1,1,1,0,0,0)$	33.6049	13.273
$(3,1,1,1,1,1,1,0,0)$	27.9202	33.587
$(2,2,2,2,1,0,0,0,0)$	23.7977	42.455
$(2,2,2,1,1,1,0,0,0)$	22.6494	34.591
$(2,2,1,1,1,1,1,0,0)$	19.7962	39.559
$(2,1,1,1,1,1,1,1,0)$	13.9854	62.802
$(1,1,1,1,1,1,1,1,1)$	0.0	100.0
$(10,0,0,0,0,0,0,0,0,0)$	100.0	100.0
$(9,1,0,0,0,0,0,0,0,0)$	93.0766	67.7441
$(8,2,0,0,0,0,0,0,0,0)$	86.1532	45.12
$(8,1,1,0,0,0,0,0,0,0)$	83.5036	41.476
$(7,3,0,0,0,0,0,0,0,0)$	79.2298	36.947
$(7,2,1,0,0,0,0,0,0,0)$	76.5802	20.739
$(7,1,1,1,0,0,0,0,0,0)$	72.6788	23.437
$(6,4,0,0,0,0,0,0,0,0)$	72.3065	39.542
$(6,3,1,0,0,0,0,0,0,0)$	69.6568	15.044
$(6,2,2,0,0,0,0,0,0,0)$	67.0072	15.044
$(6,2,1,1,0,0,0,0,0,0)$	65.7554	5.179
$(6,1,1,1,1,0,0,0,0,0)$	61.1395	14.455
$(5,5,0,0,0,0,0,0,0,0)$	65.3831	49.1901
$(5,4,1,0,0,0,0,0,0,0)$	62.7334	21.441
$(5,3,2,0,0,0,0,0,0,0)$	60.0838	13.151
$(5,3,1,1,0,0,0,0,0,0)$	58.832	3.286
$(5,2,2,1,0,0,0,0,0,0)$	56.1824	3.286
$(5,2,1,1,1,0,0,0,0,0)$	54.2161	0.0
$(5,1,1,1,1,1,0,0,0,0)$	49.2041	14.455
$(4,4,2,0,0,0,0,0,0,0)$	53.1604	24.72
$(4,4,1,1,0,0,0,0,0,0)$	51.9086	14.862
$(4,3,3,0,0,0,0,0,0,0)$	50.5108	27.307
$(4,3,2,1,0,0,0,0,0,0)$	49.259	6.572
$(4,3,1,1,1,0,0,0,0,0)$	47.2927	3.286
$(4,2,2,2,0,0,0,0,0,0)$	45.3575	14.862
$(4,2,2,1,1,0,0,0,0,0)$	44.6431	3.286
$(4,2,1,1,1,1,0,0,0,0)$	42.2807	5.179
$(4,1,1,1,1,1,1,0,0,0)$	37.0369	23.437
$(3,3,3,1,0,0,0,0,0,0)$	39.686	27.307
$(3,3,2,2,0,0,0,0,0,0)$	38.4341	24.72
$(3,3,2,1,1,0,0,0,0,0)$	37.7197	13.151
$(3,3,1,1,1,1,0,0,0,0)$	35.3573	15.044
$(3,2,2,2,1,0,0,0,0,0)$	33.8182	21.441
$(3,2,2,1,1,1,0,0,0,0)$	32.7077	15.044
$(3,2,1,1,1,1,1,0,0,0)$	30.1135	20.739
$(3,1,1,1,1,1,1,1,0,0)$	24.747	41.476
$(2,2,2,2,2,0,0,0,0,0)$	22.2789	49.1901
$(2,2,2,2,1,1,0,0,0,0)$	21.8828	39.542

λ	a_λ	b_λ
(2, 2, 2, 1, 1, 1, 1, 0, 0, 0)	20.5405	36.947
(2, 2, 1, 1, 1, 1, 1, 1, 0, 0)	17.8237	45.12
(2, 1, 1, 1, 1, 1, 1, 1, 1, 0)	12.3875	67.7441
(1, 1, 1, 1, 1, 1, 1, 1, 1, 1)	0.0	100.0
(11, 0, 0, 0, 0, 0, 0, 0, 0, 0, 0)	100.0	100.0
(10, 1, 0, 0, 0, 0, 0, 0, 0, 0, 0)	93.8295	71.265
(9, 2, 0, 0, 0, 0, 0, 0, 0, 0, 0)	87.6591	49.697
(9, 1, 1, 0, 0, 0, 0, 0, 0, 0, 0)	85.397	46.624
(8, 3, 0, 0, 0, 0, 0, 0, 0, 0, 0)	81.4886	39.924
(8, 2, 1, 0, 0, 0, 0, 0, 0, 0, 0)	79.2265	26.3731
(8, 1, 1, 1, 0, 0, 0, 0, 0, 0, 0)	75.8034	28.711
(7, 4, 0, 0, 0, 0, 0, 0, 0, 0, 0)	75.3182	39.780
(7, 3, 1, 0, 0, 0, 0, 0, 0, 0, 0)	73.0561	18.329
(7, 2, 2, 0, 0, 0, 0, 0, 0, 0, 0)	70.794	18.329
(7, 2, 1, 1, 0, 0, 0, 0, 0, 0, 0)	69.6329	10.1901
(7, 1, 1, 1, 1, 0, 0, 0, 0, 0, 0)	65.58	17.872
(6, 5, 0, 0, 0, 0, 0, 0, 0, 0, 0)	69.1477	45.913
(6, 4, 1, 0, 0, 0, 0, 0, 0, 0, 0)	66.8856	20.801
(6, 3, 2, 0, 0, 0, 0, 0, 0, 0, 0)	64.6236	12.90
(6, 3, 1, 1, 0, 0, 0, 0, 0, 0, 0)	63.4625	4.762
(6, 2, 2, 1, 0, 0, 0, 0, 0, 0, 0)	61.2004	4.762
(6, 2, 1, 1, 1, 0, 0, 0, 0, 0, 0)	59.4095	1.967
(6, 1, 1, 1, 1, 1, 0, 0, 0, 0, 0)	54.969	14.412
(5, 5, 1, 0, 0, 0, 0, 0, 0, 0, 0)	60.7152	30.394
(5, 4, 2, 0, 0, 0, 0, 0, 0, 0, 0)	58.4531	18.834
(5, 4, 1, 1, 0, 0, 0, 0, 0, 0, 0)	57.292	10.694
(5, 3, 3, 0, 0, 0, 0, 0, 0, 0, 0)	56.191	21.014
(5, 3, 2, 1, 0, 0, 0, 0, 0, 0, 0)	55.0299	2.795
(5, 3, 1, 1, 1, 0, 0, 0, 0, 0, 0)	53.2391	0.0
(5, 2, 2, 2, 0, 0, 0, 0, 0, 0, 0)	51.6068	10.694
(5, 2, 2, 1, 1, 0, 0, 0, 0, 0, 0)	50.977	0.0
(5, 2, 1, 1, 1, 1, 0, 0, 0, 0, 0)	48.7986	1.967
(5, 1, 1, 1, 1, 1, 1, 0, 0, 0, 0)	44.1465	17.872
(4, 4, 3, 0, 0, 0, 0, 0, 0, 0, 0)	50.0206	31.70
(4, 4, 2, 1, 0, 0, 0, 0, 0, 0, 0)	48.8595	13.4
(4, 4, 1, 1, 1, 0, 0, 0, 0, 0, 0)	47.0686	10.694
(4, 3, 3, 1, 0, 0, 0, 0, 0, 0, 0)	46.5974	15.6
(4, 3, 2, 2, 0, 0, 0, 0, 0, 0, 0)	45.4363	13.4
(4, 3, 2, 1, 1, 0, 0, 0, 0, 0, 0)	44.8065	2.795
(4, 3, 1, 1, 1, 1, 0, 0, 0, 0, 0)	42.6281	4.762
(4, 2, 2, 2, 1, 0, 0, 0, 0, 0, 0)	41.3834	10.694
(4, 2, 2, 1, 1, 1, 0, 0, 0, 0, 0)	40.366	4.762
(4, 2, 1, 1, 1, 1, 1, 0, 0, 0, 0)	37.9761	10.1901
(4, 1, 1, 1, 1, 1, 1, 1, 0, 0, 0)	33.1883	28.711
(3, 3, 3, 2, 0, 0, 0, 0, 0, 0, 0)	37.0038	31.70
(3, 3, 3, 1, 1, 0, 0, 0, 0, 0, 0)	36.374	21.014
(3, 3, 2, 2, 1, 0, 0, 0, 0, 0, 0)	35.2129	18.834
(3, 3, 2, 1, 1, 1, 0, 0, 0, 0, 0)	34.1956	12.90
(3, 3, 1, 1, 1, 1, 1, 0, 0, 0, 0)	31.8056	18.329
(3, 2, 2, 2, 2, 0, 0, 0, 0, 0, 0)	31.1599	30.394
(3, 2, 2, 2, 1, 1, 0, 0, 0, 0, 0)	30.7724	20.801
(3, 2, 2, 1, 1, 1, 1, 0, 0, 0, 0)	29.5435	18.329
(3, 2, 1, 1, 1, 1, 1, 1, 0, 0, 0)	27.0179	26.3731
(3, 1, 1, 1, 1, 1, 1, 1, 1, 0, 0)	22.1582	46.624
(2, 2, 2, 2, 2, 1, 0, 0, 0, 0, 0)	20.549	45.913
(2, 2, 2, 2, 1, 1, 1, 0, 0, 0, 0)	19.9499	39.780
(2, 2, 2, 1, 1, 1, 1, 1, 0, 0, 0)	18.5853	39.924
(2, 2, 1, 1, 1, 1, 1, 1, 1, 0, 0)	15.9878	49.697
(2, 1, 1, 1, 1, 1, 1, 1, 1, 1, 0)	11.0873	71.265
(1, 1, 1, 1, 1, 1, 1, 1, 1, 1, 1)	0.0	100.0
(12, 0, 0, 0, 0, 0, 0, 0, 0, 0, 0, 0)	100.0	100.0
(11, 1, 0, 0, 0, 0, 0, 0, 0, 0, 0, 0)	94.5958	74.832
(10, 2, 0, 0, 0, 0, 0, 0, 0, 0, 0, 0)	89.1916	54.707

λ	a_λ	b_λ
(10, 1, 1, 0, 0, 0, 0, 0, 0, 0, 0, 0)	87.0838	52.743
(9, 3, 0, 0, 0, 0, 0, 0, 0, 0, 0, 0)	83.7874	43.844
(9, 2, 1, 0, 0, 0, 0, 0, 0, 0, 0, 0)	81.6796	33.490
(9, 1, 1, 1, 0, 0, 0, 0, 0, 0, 0, 0)	78.5079	35.703
(8, 4, 0, 0, 0, 0, 0, 0, 0, 0, 0, 0)	78.3831	41.257
(8, 3, 1, 0, 0, 0, 0, 0, 0, 0, 0, 0)	76.2754	23.775
(8, 2, 2, 0, 0, 0, 0, 0, 0, 0, 0, 0)	74.1676	23.775
(8, 2, 1, 1, 0, 0, 0, 0, 0, 0, 0, 0)	73.1037	17.598
(8, 1, 1, 1, 1, 0, 0, 0, 0, 0, 0, 0)	69.3148	24.48
(7, 5, 0, 0, 0, 0, 0, 0, 0, 0, 0, 0)	72.9789	44.246
(7, 4, 1, 0, 0, 0, 0, 0, 0, 0, 0, 0)	70.8711	22.913
(7, 3, 2, 0, 0, 0, 0, 0, 0, 0, 0, 0)	68.7634	15.785
(7, 3, 1, 1, 0, 0, 0, 0, 0, 0, 0, 0)	67.6995	9.608
(7, 2, 2, 1, 0, 0, 0, 0, 0, 0, 0, 0)	65.5917	9.608
(7, 2, 1, 1, 1, 0, 0, 0, 0, 0, 0, 0)	63.9106	8.104
(7, 1, 1, 1, 1, 1, 0, 0, 0, 0, 0, 0)	59.7695	18.845
(6, 6, 0, 0, 0, 0, 0, 0, 0, 0, 0, 0)	67.5747	50.894
(6, 5, 1, 0, 0, 0, 0, 0, 0, 0, 0, 0)	65.4669	28.138
(6, 4, 2, 0, 0, 0, 0, 0, 0, 0, 0, 0)	63.3591	17.15
(6, 4, 1, 1, 0, 0, 0, 0, 0, 0, 0, 0)	62.2953	10.981
(6, 3, 3, 0, 0, 0, 0, 0, 0, 0, 0, 0)	61.2514	19.530
(6, 3, 2, 1, 0, 0, 0, 0, 0, 0, 0, 0)	60.1875	3.854
(6, 3, 1, 1, 1, 0, 0, 0, 0, 0, 0, 0)	58.5064	2.350
(6, 2, 2, 2, 0, 0, 0, 0, 0, 0, 0, 0)	57.0159	10.981
(6, 2, 2, 1, 1, 0, 0, 0, 0, 0, 0, 0)	56.3986	2.350
(6, 2, 1, 1, 1, 1, 0, 0, 0, 0, 0, 0)	54.3653	4.700
(6, 1, 1, 1, 1, 1, 1, 0, 0, 0, 0, 0)	49.9969	18.845
(5, 5, 2, 0, 0, 0, 0, 0, 0, 0, 0, 0)	57.9549	25.7881
(5, 5, 1, 1, 0, 0, 0, 0, 0, 0, 0, 0)	56.8911	19.6111
(5, 4, 3, 0, 0, 0, 0, 0, 0, 0, 0, 0)	55.8471	24.3081
(5, 4, 2, 1, 0, 0, 0, 0, 0, 0, 0, 0)	54.7833	8.631
(5, 4, 1, 1, 1, 0, 0, 0, 0, 0, 0, 0)	53.1022	7.127
(5, 3, 3, 1, 0, 0, 0, 0, 0, 0, 0, 0)	52.6755	11.003
(5, 3, 2, 2, 0, 0, 0, 0, 0, 0, 0, 0)	51.6117	8.631
(5, 3, 2, 1, 1, 0, 0, 0, 0, 0, 0, 0)	50.9944	0.0
(5, 3, 1, 1, 1, 1, 0, 0, 0, 0, 0, 0)	48.9611	2.350
(5, 2, 2, 2, 1, 0, 0, 0, 0, 0, 0, 0)	47.8227	7.127
(5, 2, 2, 1, 1, 1, 0, 0, 0, 0, 0, 0)	46.8533	2.350
(5, 2, 1, 1, 1, 1, 1, 0, 0, 0, 0, 0)	44.5927	8.104
(5, 1, 1, 1, 1, 1, 1, 1, 0, 0, 0, 0)	40.099	24.48
(4, 4, 4, 0, 0, 0, 0, 0, 0, 0, 0, 0)	48.3351	38.25
(4, 4, 3, 1, 0, 0, 0, 0, 0, 0, 0, 0)	47.2713	19.634
(4, 4, 2, 2, 0, 0, 0, 0, 0, 0, 0, 0)	46.2074	17.2631
(4, 4, 2, 1, 1, 0, 0, 0, 0, 0, 0, 0)	45.5902	8.631
(4, 4, 1, 1, 1, 1, 0, 0, 0, 0, 0, 0)	43.5569	10.981
(4, 3, 3, 2, 0, 0, 0, 0, 0, 0, 0, 0)	44.0997	19.634
(4, 3, 3, 1, 1, 0, 0, 0, 0, 0, 0, 0)	43.4824	11.003
(4, 3, 2, 2, 1, 0, 0, 0, 0, 0, 0, 0)	42.4185	8.631
(4, 3, 2, 1, 1, 1, 0, 0, 0, 0, 0, 0)	41.4491	3.854
(4, 3, 1, 1, 1, 1, 1, 0, 0, 0, 0, 0)	39.1885	9.608
(4, 2, 2, 2, 2, 0, 0, 0, 0, 0, 0, 0)	38.6296	19.6111
(4, 2, 2, 2, 1, 1, 0, 0, 0, 0, 0, 0)	38.2774	10.981
(4, 2, 2, 1, 1, 1, 1, 0, 0, 0, 0, 0)	37.0807	9.608
(4, 2, 1, 1, 1, 1, 1, 1, 0, 0, 0, 0)	34.6948	17.598
(4, 1, 1, 1, 1, 1, 1, 1, 1, 0, 0, 0)	30.1207	35.703
(3, 3, 3, 3, 0, 0, 0, 0, 0, 0, 0, 0)	35.5238	38.25
(3, 3, 3, 2, 1, 0, 0, 0, 0, 0, 0, 0)	34.9065	24.3081
(3, 3, 3, 1, 1, 1, 0, 0, 0, 0, 0, 0)	33.9371	19.530
(3, 3, 2, 2, 2, 0, 0, 0, 0, 0, 0, 0)	33.2254	25.7881
(3, 3, 2, 2, 1, 1, 0, 0, 0, 0, 0, 0)	32.8732	17.15
(3, 3, 2, 1, 1, 1, 1, 0, 0, 0, 0, 0)	31.6765	15.785
(3, 3, 1, 1, 1, 1, 1, 1, 0, 0, 0, 0)	29.2906	23.775
(3, 2, 2, 2, 2, 1, 0, 0, 0, 0, 0, 0)	29.0843	28.138

λ	a_λ	b_λ
(3, 2, 2, 2, 1, 1, 1, 0, 0, 0, 0, 0)	28.5049	22.913
(3, 2, 2, 1, 1, 1, 1, 1, 0, 0, 0, 0)	27.1828	23.775
(3, 2, 1, 1, 1, 1, 1, 1, 1, 0, 0, 0)	24.7165	33.490
(3, 1, 1, 1, 1, 1, 1, 1, 1, 1, 0, 0)	20.0998	52.743
(2, 2, 2, 2, 2, 2, 0, 0, 0, 0, 0, 0)	19.539	50.894
(2, 2, 2, 2, 2, 1, 1, 0, 0, 0, 0, 0)	19.3117	44.246
(2, 2, 2, 2, 1, 1, 1, 1, 0, 0, 0, 0)	18.6069	41.257
(2, 2, 2, 1, 1, 1, 1, 1, 1, 0, 0, 0)	17.2045	43.844
(2, 2, 1, 1, 1, 1, 1, 1, 1, 1, 0, 0)	14.6956	54.707
(2, 1, 1, 1, 1, 1, 1, 1, 1, 1, 1, 0)	10.0548	74.832
(1, 1, 1, 1, 1, 1, 1, 1, 1, 1, 1, 1)	0.0	100.0

Acknowledgments

The author is grateful to Alex Davies and Been Kim for their helpful discussions. He also thanks the anonymous referee whose comments significantly improved the exposition of this paper. The author would like to acknowledge the support and hospitality of the Isaac Newton Institute for Mathematical Sciences and the Center for Quantum Structures in Modules and Spaces.

Funding

This work was partially supported by an EPSRC grant #EP/R014604/1 and by a grant from the Simons Foundation (#712100).

References

[1] Ashmore, A., He, Y.-H., Ovrut, B. A. Machine learning Calabi–Yau metrics. arXiv:1910.08605 [hep-th].
[2] Ballantine, C. M., Orellana, R. C. (2006). A combinatorial interpretation for the coefficients in the Kronecker product $s_{(n-p,p)} * s_\lambda$. *Sém. Lothar. Combin.* 54A:Art. B54Af, 29.
[3] Blasiak, J., Mulmuley, K. D., Sohoni, M. (2015). *Geometric Complexity Theory IV: Nonstandard Quantum Group for the Kronecker Problem*. Memoirs of the American Mathematical Society, Vol. 235, no. 1109. Providence, RI: American Mathematical Society.
[4] Blasiak, J. (2012). An insertion algorithm for catabolizability. *Eur. J. Combin.* 33(2): 267–276.
[5] Buzzard, K. What is the point of computers? A question for pure mathematicians. arXiv:2112.11598.
[6] Carifio, J., Halverson, J., Krioukov, D., Nelson, B. D. (2017). Machine learning in the string landscape. *JHEP* 2017:157.
[7] Davies, A., Veličković, P., Buesing, L., Blackwell, S., Zheng, D., Tomašev, N., Tanburn, R., Battaglia, P., Blundell, C., Juhász, A., Lackenby, M., Williamson, G., Hassabis, D., Kohli, P. (2021). Advancing mathematics by guiding human intuition with AI. *Nature* 600:70–74.
[8] Douglas, M., Lakshminarasimhan, S., Qi, Y. (2022). Numerical Calabi–Yau metrics from holomorphic networks. *Proc. Mach. Learn. Res.* 145:223–252.
[9] Fulton, W., Harris, J. (1991). *Representation Theory*. Graduate Texts in Mathematics, 129. New York: Springer-Verlag.
[10] Gantmacher, F. (1959). *Applications of the Theory of Matrices*. Interscience Publishers.
[11] Hastie, T., Tibshirani, R., Friedman, J. (2001). *The Elements of Statistical Learning: Data Mining, Inference, and Prediction*. New York: Springer.
[12] He, Y.-H., Kim, M. Learning algebraic structures: preliminary investigations, arXiv:1905.02263 [cs.LG].
[13] He, Y.-H., Lee, K.-H., Oliver, T. (2022). Machine-learning the Sato–Tate conjecture. *J. Symb. Comput.* 111:61–72.
[14] He, Y.-H., Lee, K.-H., Oliver, T. (2022). Machine-learning number fields. *Math. Comput. Geom. Data* 2: 49–66.
[15] He, Y.-H., Lee, K.-H., Oliver, T. (2023). Machine learning invariants of arithmetic curves. *J. Symb. Comput.* 115: 478–491.
[16] He, Y.-H., Lee, K.-H., Oliver, T., Pozdnyakov, A. (2024). Murmurations of elliptic curves. *Exp. Math*. DOI: 10.1080/10586458.2024.2382361.
[17] Ikenmeyer, C., Mulmuley, K. D., Walter, M. (2017). On vanishing of Kronecker coefficients. *Comput. Complex.* 26: 949–992.
[18] James, G., Kerber, A. (1981). *The Representation Theory of the Symmetric Group*. Encyclopedia of Mathematics and its Applications, 16. Reading, MA: Addison-Wesley Publishing Co.
[19] Jejjala, V., Kar, A., Parrikar, O. (2019). Deep learning the hyperbolic volume of a knot. *Phys. Lett. B* 799: 135033.
[20] Lee, K.-H. (2024). Machine-learning Kronecker coefficients. *Int. J. Data Sci. Math. Sci.* 2(1): 79–86.
[21] Murnaghan, D. (1938). The analysis of the Direct product of irreducible representations of the symmetric groups. *Amer. J. Math.* 60(9): 44–65.
[22] Pak, I., Panova, G. (2017). Bounds on certain classes of Kronecker and q-binomial coefficients. *J. Combin. Theory Ser. A* 147: 1–17.
[23] (2017). On the complexity of computing Kronecker coefficients. *Comput. Complexity* 26(1): 1–36.
[24] Remmel, J. B. (1989). A formula for the Kronecker products of Schur functions of hook shapes. *J. Algebra* 120: 100–118.
[25] Remmel, J. B., Whitehead, T. (1994). On the Kronecker product of Schur functions of two row shapes. *Bull. Belg. Math. Soc. Simon Stevin* 1: 649–683.
[26] Ressayre, N. (2019). Horn inequalities for nonzero Kronecker coefficients. *Adv. Math.* 356: 106809.
[27] Williamson, G. Is deep learning a useful tool for the pure mathematician? arXiv:2304.12602.